International Journal of Bifurcation and Chaos, Vol. 13, No. 7 (2003) 1767–1785

ON THE FRACTAL STRUCTURE OF BASIN BOUNDARIES IN TWO-DIMENSIONAL NONINVERTIBLE MAPS

A. AGLIARI
Catholic University of Milano, Largo Gemelli 1, 20123 Milano, Italy
agliari@unipr.it

L. GARDINI
University of Urbino, 61029 Urbino, Italy
gardini@econ.uniurb.it

C. MIRA
19 rue d'Occitanie, Fonsegrives, 31130 Quint,
Toulouse Cedex, France
christian.mira@insa-tlse.fr

Received December 10, 2000; Revised October 25, 2001

In this paper we give an example of transition to fractal basin boundary in a two-dimensional map coming from the applicative context, in which the hard-fractal structure can be rigorously proved. That is, not only via numerical examples, although theoretically guided, as often occurs in maps coming from the applications, but also via analytical tools. The proposed example connects the two-dimensional maps of the real plane to the well-known complex map.

Keywords: Basin bifurcation; fractalization; Julia set; noninvertible map.

1. Introduction

The object of the work is to show an example of fractalization of a basin boundary in a two-dimensional noninvertible map, which gives a kind of link, or connection, with the well known complex map

$$z' = z^2 + C \quad z \in \mathbb{C}$$

The example we shall deal with comes from the applicative field. It models the mean equity ratio a and its variance V, useful to study the financial robustness of the firms, in an economic environment. It was proposed two years ago in our economic department. Independent of the meaning of the variables, $(a, V) = (x, y)$, the two-dimensional map modeling the dynamics of the financial processes reads as

$$\begin{cases} x' = -g_0 + g_1 x - g_2 x^2 - g_2 y \\ y' = g_2^2(\beta - 1)y^2 + (2g_2 x - g_1)^2 y \\ \qquad + 4g_2^2 g_3 x - 2g_1 g_2 g_3 \end{cases} \tag{1}$$

It was published in [Agliari *et al.*, 2000], and in the same paper the usual properties of local stability were reported as well as some considerations on the global dynamics and global bifurcations, following the properties of noninvertible maps as described in the references [Gumowski & Mira, 1980a, 1980b; Mira *et al.*, 1996; Abraham *et al.*, 1997].

The case in which $g_3 = 0$ in (1) is particularly important because the map has the x-axis trapping and it corresponds to the existence of a "representative agent". We shall restrict our analysis to this

case:

$$F : \begin{cases} x' = -g_0 + g_1 x - g_2 x^2 - g_2 y \\ y' = g_2^2(\beta - 1)y^2 + (2g_2 x - g_1)^2 y \end{cases} \tag{2}$$

In the paper [Agliari *et al.*, 2000] we have reported some dynamic properties also for the map F. In particular Figs. 1 and 2, related to $\beta = 1$ and $\beta > 1$ have been explained in terms of the asymptotic properties of the attracting sets, and the properties of two-dimensional noninvertible maps.

It is clear that the suggestive behavior of the basin in the region of negative y, say

$$\Pi_- = \{(x, y) \in \mathbb{R}^2 : y < 0\}, \tag{3}$$

recalls the behavior of the complex map

$$z' = z^2 + C \quad z = (x, y) \in \mathbb{C} \tag{4}$$

where the parameter C in our analysis is to be considered real, i.e. $C = (-c, 0)$.

In terms of a two-dimensional real map, (4) reads as

$$Z : \begin{cases} x' = x^2 - y^2 - c \\ y' = 2xy \end{cases} \tag{5}$$

At a first glance it seems quite far from our model (2), while we shall see that when $\beta = 1$, F is *semi-conjugate* to (5).

The plan of the work is as follows. In Sec. 2 we shall introduce new coordinates which allow us to rewrite the map F in a more suitable form, and we shall describe the foliation of the real plane for the new model T, topologically conjugated with F. In Sec. 3.1 we shall prove that for $\beta = 1$ the frontier of the basin in the half-plane Π_- has a true hard-fractal structure, following the definitions given in [Mira *et al.*, 1994] and [Mira *et al.*, 1996], as F is *semi-conjugate* to the complex map (5). In Sec. 3.2 we shall describe the transition to half-fractal basin occurring for $\beta > 1$ proving the persistence of infinitely many cycles, of any order, belonging to the negative half-plane Π_-, while in Sec. 3.3 we shall see how the hard-fractal structure of the basin boundary is reached starting from a smooth frontier, at increasing values of β for $\beta < 1$.

2. Change of Coordinates and Structure of the Foliation

In this section we first rewrite our economic model in a more suitable form, from the mathematical point of view. We introduce the change of variable

$$h : \begin{cases} x = \dfrac{1}{g_2}\left(\dfrac{g_1}{2} - X\right) \\ y = \dfrac{Y}{g_2^2} \end{cases} \tag{6}$$

Being $h(X, Y)$ a diffeomorphism, we have that the map (2) is topologically conjugate to $T = h \circ F \circ h^{-1}$, which only depends on two parameters $c = -(4g_0 g_2 + 2g_1 - g_1^2)/4$ and β. In fact, applying the change of coordinates (6) to (2) and writing (x, y) instead of (X, Y), we obtain the map

$$T : \begin{cases} x' = x^2 + y - c \\ y' = (\beta - 1)y^2 + 4x^2 y \end{cases} \tag{7}$$

The transition $\beta < 1$, $\beta = 1$, $\beta > 1$ characterizes an important bifurcation of the basin boundary.

Let us denote by B_∞ the set of points of the phase plane having divergent trajectories. Its complementary set is the set of points having bounded trajectories belonging to some frontier or to some basin of attraction and thus convergent to some attracting set (and in this map we have that the multistability is the generic situation, see [Agliari *et al.*, 2000]).

The map T has the x-axis which is trapping and the restriction of T to that axis reduces to the well-known Myrberg's map (conjugate to the logistic map)

$$x' = x^2 - c$$

and also the structure of the foliation of T is clear. We recall that by *Riemann foliation of the plane* we mean, following the literature on noninvertible maps (see [Gumowski & Mira, 1980b; Mira *et al.*, 1996]), the understanding of the superimposed "sheets" which cover the plane giving reason to the number of preimages existing in its different parts. In fact, the Jacobian of T is given by

$$J(x, y) = \begin{bmatrix} 2x & 1 \\ 8xy & 2(\beta - 1)y + 4x^2 \end{bmatrix}$$

whose determinant $|J(x, y)| = 4x(y\beta - 3y + 2x^2)$ vanishes on two curves, here denoted as $LC_{-1}^{(a)}$ and $LC_{-1}^{(b)}$, given by

$$\begin{cases} LC_{-1}^{(a)} : x = 0 \\ LC_{-1}^{(b)} : y = -\dfrac{2x^2}{\beta - 3} \end{cases} \tag{8}$$

where it is assumed $\beta \neq 3$, as in fact, in this paper we are interested in the range $\beta < 3$.

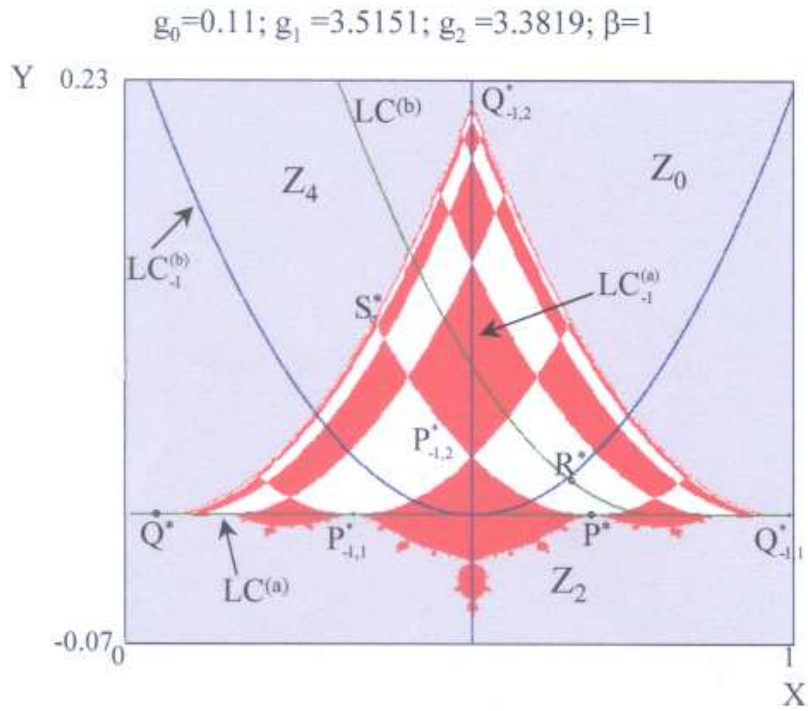

(a)

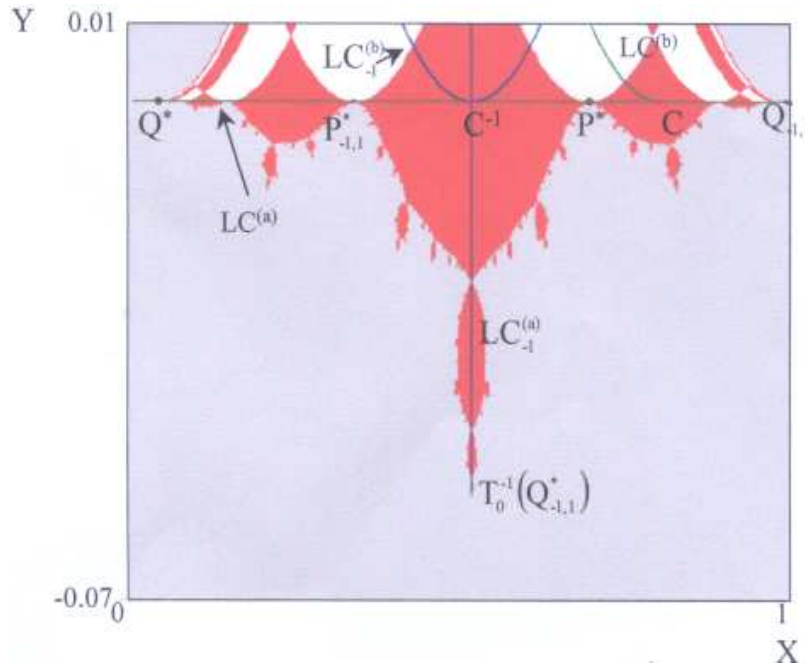

(b)

Fig. 1. (a) An example of dynamic behavior of the economic model F, obtained for $\beta = 1$. The map F has four fixed points, two of them repelling, Q^* and S^*, always located on the frontier of the basin of bounded trajectories (not gray points). In the case represented, the attracting sets are the fixed point R^* and a 2-cycle, on the invariant axis x, born via flip bifurcation of P^*. The set of points having trajectories converging to R^* is denoted in white and the one of points converging to the 2-cycle in red. The separation point between the two basins are the preimages of any rank of P^*, which belongs to Z_4 (only those of rank-1 are marked in figure). Also the *Riemann foliation* of the map F is represented in the same figure. (b) In the enlargement, the region of negative y, Π_-, is shown: in such a region, all the points with converging trajectories go to the 2-cycles. The frontier of the basins of attraction of the 2-cycle in Π_- seems to have a fractal structure.

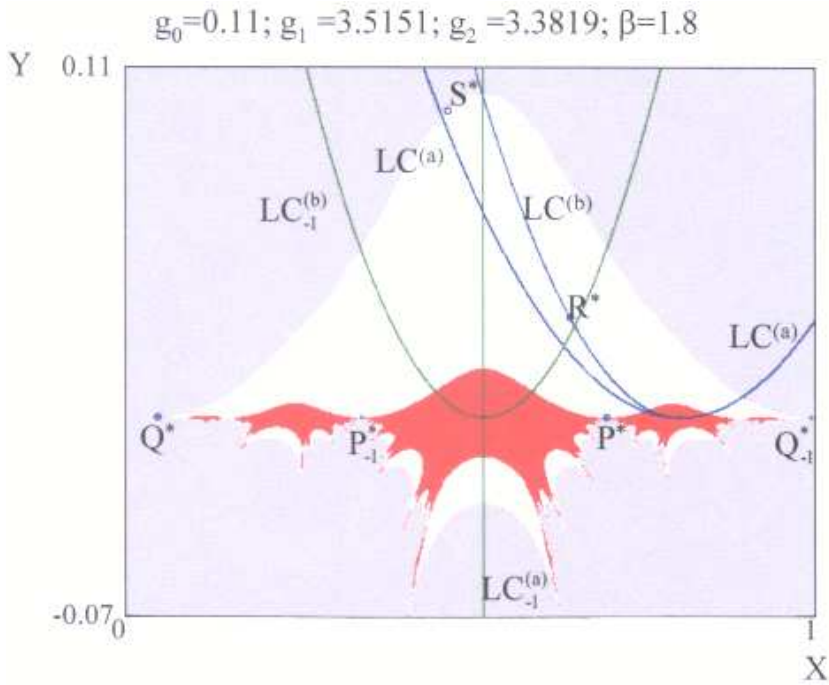

(a)

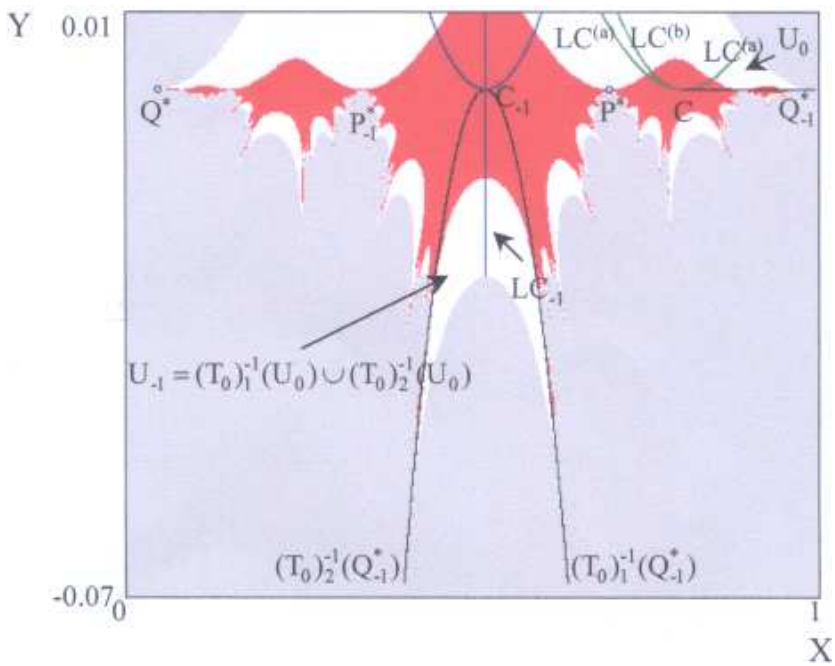

(b)

Fig. 2. (a) An example of dynamic behavior of the economic model F, obtained for $\beta > 1$. The attracting sets are the same as in Fig. 1, but their basins of attraction (always denoted in white and red) now are quite different. This is due to the different *Riemann foliation* of the map: the region Z_4 now is smaller with respect to the previous case, the fixed point P^* belongs to the Z_2 region and the preimages are in Π_-. (b) In the enlargement we can observe also the different behavior of the points of Π_-. In fact, now, there are also white points, which are the preimages of any rank of the region U_0 (a small subset of the region of positive y belonging to Z_2). As a consequence the frontier of the set of points having unbounded trajectories (gray points) seems to have a half-fractal structure.

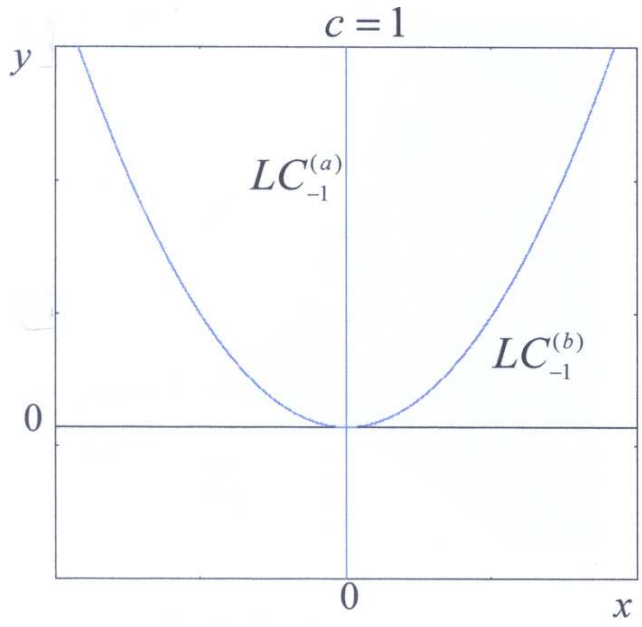

(a)

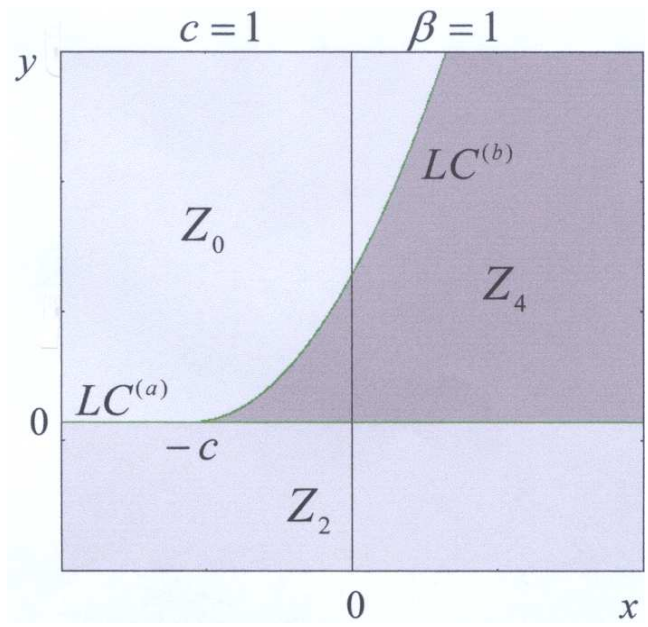

(b)

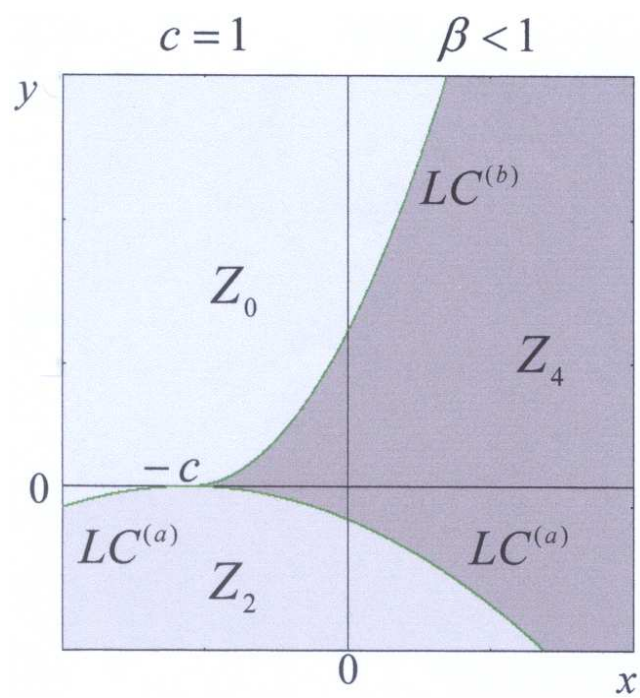

(c)

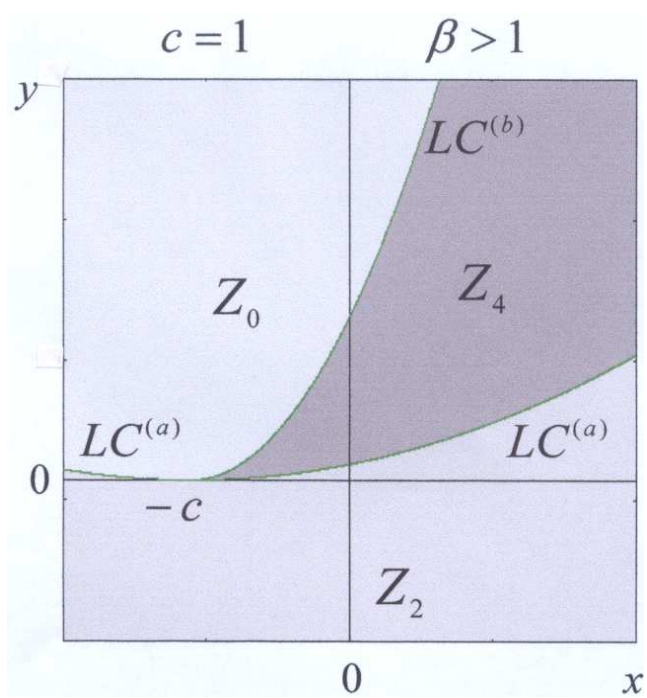

(d)

Fig. 3. Critical sets and *Riemann foliation* of the map T. (a) The two curves LC_{-1}, the locus of points of the phase plane (x, y) in which the determinant of the Jacobian matrix of T vanishes. (b) Case $\beta = 1$. The critical set $LC = T(LC_{-1})$, locus of points with merging preimages, is given by the x-axis ($LC^{(a)}$) and an half parabola ($LC^{(b)}$) located in Π_+ with vertex $(-c, 0)$. The region Z_0 is at the left of $LC^{(b)}$ and Z_4 at the right. The region Z_2 coincides with Π_-, which is an invariant set, i.e. $T(\Pi_-) = \Pi_-$, for T. (c) Case $\beta < 1$. $LC^{(b)}$ is similar to the previous case, but $LC^{(a)}$ now is a parabola in the half plane Π_-, with vertex in $(-c, 0)$. Thus the region Z_4 is increased and the region Z_2 is smaller. Now Π_- is a traffing set, i.e. $T(\Pi_-) \subset \Pi_-$. (d) Case $\beta > 1$. The region Z_4 is smaller than in the previous cases, because $LC^{(b)}$ is a parabola of the half-plane Π_+ and Z_2 is larger. Now $T(\Pi_-) \supset \Pi_-$.

The images by T of (8) give the critical curve LC of the map, made up of two branches, which separate regions of the phase plane having different number of rank-1 preimages. These regions are denoted by Z_i, where i denotes the number of distinct rank-1 preimages of any point in the region.

We obtain

$$\begin{cases} LC^{(a)} : y = (\beta - 1)(x + c)^2 \\ LC^{(b)} : \begin{cases} y = \dfrac{4}{5 - \beta}(x + c)^2 \\ x \geq c \end{cases} \end{cases}$$

Determining the inverses by solving the system

$$\begin{cases} x' = x^2 + y - c \\ y' = (\beta - 1)y^2 + 4x^2 y \end{cases}$$

with respect to (x, y), it is easy to see that the map T is of so-called type $Z_0 - Z_2 - Z_4$ and the structure of the foliation depends on the value of the parameter β. The two curves giving LC_{-1} are shown in Fig. 3(a) while the two branches of the critical curve LC are shown in Figs. 3(b)–3(d).

In particular, a Z_0 region always exists and a Z_4 region decreases as β increases. There is an important qualitative change as β crosses 1. In fact, the critical curve $LC^{(a)}$ is a parabola in the half-plane Π_- for $\beta < 1$, while it is located in Π_+ for $\beta > 1$ and it degenerates, reducing to the x-axis, for $\beta = 1$, i.e. $LC^{(a)} = \{y = 0\}$ for $\beta = 1$. At the same time, the properties of the region Z_2 in the half-plane Π_- also changes as β crosses 1. For $\beta < 1$ we see that $T(\Pi_-) \subset \Pi_-$, i.e. the negative half-plane is trapping, while at $\beta = 1$ we have $T(\Pi_-) = \Pi_-$, i.e. the negative half-plane is invariant and, for $\beta > 1$, $T(\Pi_-) \supset \Pi_-$, so that it is no longer trapping.

But an important property persists for $\beta = 1$ as well as for $\beta > 1$: the whole region Π_- belongs to Z_2 and as we shall see, any point $P \in \Pi_-$ has two distinct rank-1 preimages belonging to the same half-plane, one on the right of the y-axis (which is $LC^{(a)}_{-1}$) and one on the left of the y-axis:

$$P \in \Pi_- \Rightarrow T_R^{-1}(P) \in \Pi_-$$

$$\text{and} \quad T_L^{-1}(P) \in \Pi_-$$

and this will characterize the particular dynamic behavior of the map in the negative half-plane. It is also easy to write in explicit form these two inverses. For any point $P = (u, v) \in \Pi_-$ we have

$$T_R^{-1}(u, v) = (\sqrt{u + c - \xi}, \xi)$$

$$T_L^{-1}(u, v) = (-\sqrt{u + c - \xi}, \xi)$$

where

$$\xi = \frac{2(u + c) - \sqrt{4(u + c)^2 + |v|(5 - \beta)}}{(5 - \beta)}$$

3. Frontier of the Basin

Let us now turn to the dynamic behaviors of T. We only deal with the properties of the basin boundary ∂B_∞, referring to the paper [Agliari *et al.*, 2000] for other kind of details, as the bifurcations of the fixed points. We are interested in the transition of the basin as β crosses through 1. The values of the parameter c governs the dynamics on the x-axis, and here we shall only consider two values of c, $c = 0.65$ for which the fixed point P^* on the x-axis is attracting, and $c = 1$, after the flip bifurcation of P^* (which is a bifurcation with double eigenvalue equal to 1 for the two-dimensional map T). When $c = 1$ the attracting set on the x-axis is the 2-cycle $\{(0, 0), (-1, 0)\}$, in the supercritical situation (one of the eigenvalues of the two cycle is zero, and in fact one point is a critical point belonging to LC_{-1}). However this value has been chosen only because the Julia set of the complex map with real parameter -1, i.e. $z' = z^2 - 1$, is well known, but any other value of c in the range $(0.75, 1.25)$ (interval of existence of an attracting 2-cycle on the x-axis) works well.

For $c = 1$ beside the attracting 2-cycle on the x-axis, there exists a stable fixed point R^* in the positive half-plane Π_+. The basin of the 2-cycle is represented in red in Fig. 4 and in the following, while the basin of the fixed point R^* is represented in white.

3.1. *Case* $\beta = 1$

Let us consider our map T in the particular case $\beta = 1$. It reads

$$T_1 : \begin{cases} x' = x^2 + y - c \\ y' = 4x^2 y \end{cases} \tag{9}$$

and comparing it with the complex map Z given in (5) we can see, from Figs. 4 and 5, that a strict connection exists, in fact the basin boundary of T_1 in the negative half-plane Π_- is not only "similar" to that of the complex map Z, as stated in the following proposition.

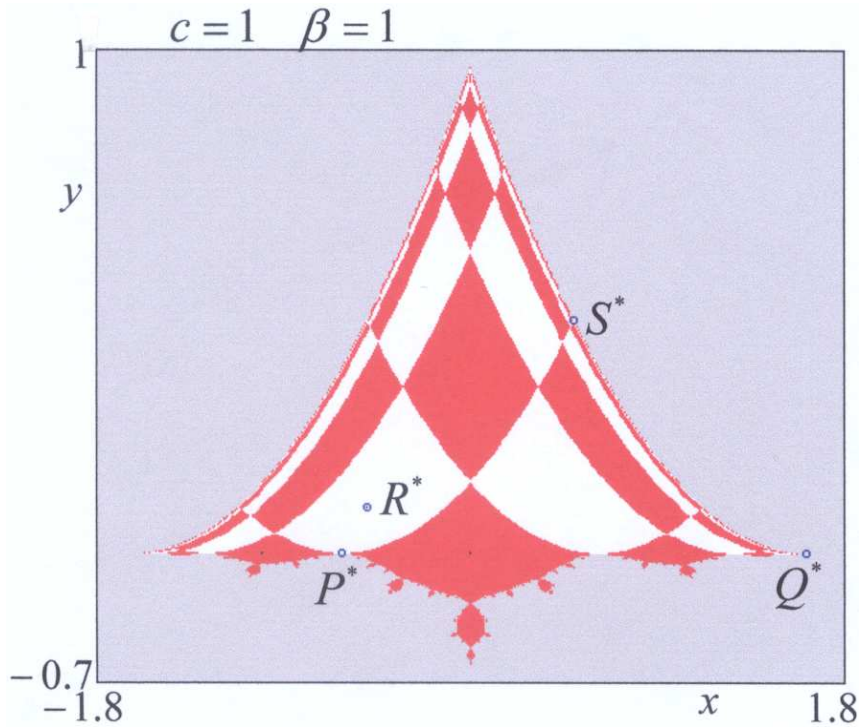

(a)

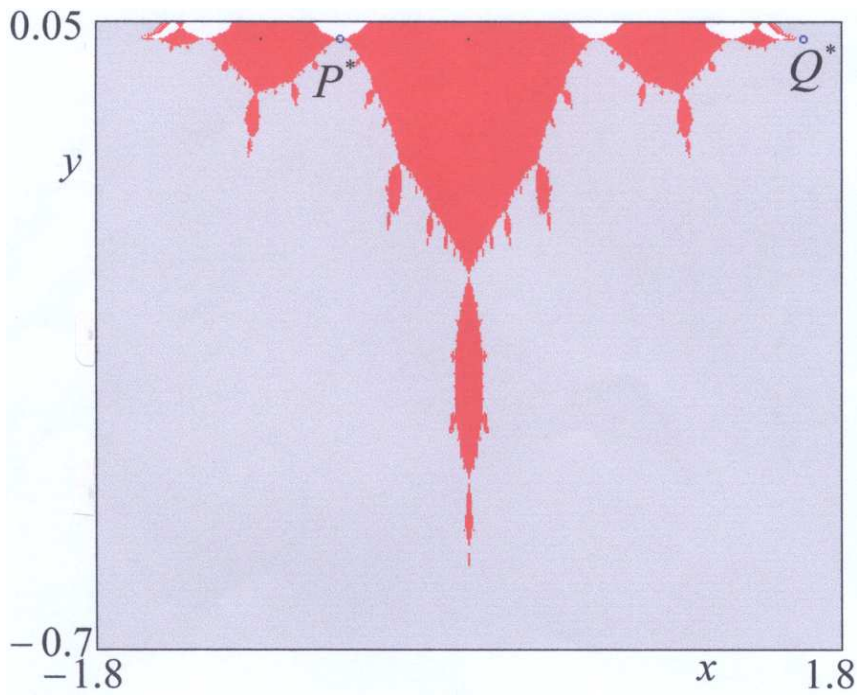

(b)

Fig. 4. (a) The set of points with bounded trajectories for the map T, when $c = 1$ and $\beta = 1$: the attractors are the fixed point R^* (its basin of attraction, $\mathcal{B}(R^*)$, is given in white) and a 2-cycle on the x-axis (with basin of attraction, $\mathcal{B}$(2-cycle), the red points). P^*, S^* and Q^* are repelling fixed points. (b) In the enlargement only Π_- is shown and the "hard-fractal" structure of the boundary of $\mathcal{B}$(2-cycle) is more evident.

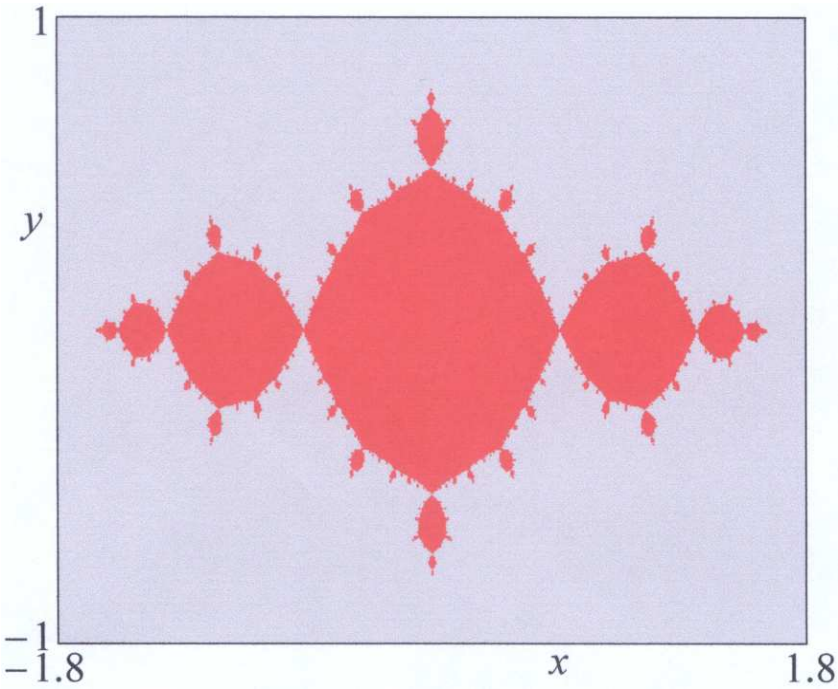

Fig. 5. The Julia set of the complex map $z' = z^2 - 1$. A strict connection with Fig. 4(b) exists, due to the semi-conjugacy between the two maps.

Proposition. The map T_1 *in* (9) *restricted on the negative half-plane is semiconjugate to the map* Z *in* (5) *given on* $\mathbb{R}^2$, *namely* $T_1 \circ h_1 = h_1 \circ Z$, *where* $h_1(x, y) = (x, -y^2)$.

Proof. $T_1 \circ h_1(x, y) = T_1(x, -y^2) = (x^2 - y^2 - c, -4x^2y^2)$.

$h_1 \circ Z(x, y) = h_1(x^2 - y^2 - c, 2xy) = (x^2 - y^2 - c, -4x^2y^2)$. ■

Thus when $\beta = 1$ our map is really connected with the complex map, although only in the negative half-plane Π_-.

Transferring the properties of the complex map to our map T_1 we have on the frontier $\mathcal{F} \subset \Pi_-$ infinitely many cycles of any order, all expanding (repelling nodes or foci).

The upper part of $\mathcal{F} \subset \Pi_+$ has not the same property, really it depends on the values of the parameters c, and at $c = 1$ it seems smooth: there is another fixed point S^*, saddle, whose stable set reaches Q^* (the other repelling fixed point of the Myrberg's map, on the x-axis) on one side, and LC on the other side, giving rise to the smooth bell-shaped basin boundary. While below the x-axis the red basin of the two cycle has a so-called "hard-fractal" boundary, which is nowhere differentiable.

The other portions of the red basin in the positive region Π_+ are well explained following the critical curve properties and the foliation structure. This basin in the half-plane $y > 0$ may be considered disconnected, made up of infinitely many components of "quadrilateral shape", but with connected closure, and the points connecting these portions, the extrema of the quadrilateral regions, are all *preimages of any rank of the repelling fixed point* P^*. This fixed point has one rank-1 preimage in itself, another rank-1 preimage on the a-axis, called $P^*_{-1,1}$ in Fig. 1, and two merging rank-1 preimages in the point $P^*_{-1,2}$ of $LC^{(a)}_{-1}$. This last point is internal to Z_4 and thus has four distinct rank-1 preimages, all in the half-plane Π_+, and so on.

3.2. *Case* $\beta > 1$

The pure fractal structure of the two-dimensional map T only exist for $\beta = 1$, and it is destroyed for $\beta > 1$ or $\beta < 1$, and this allows us to show the so-called route (or transition) to fractal structure which, in two-dimensional real maps, is generally a "half-fractal" structure, following the description given in [Mira *et al.*, 1996]. The half-fractal structure means that there exist smooth arcs on the frontier, but following a fractal structure, typical

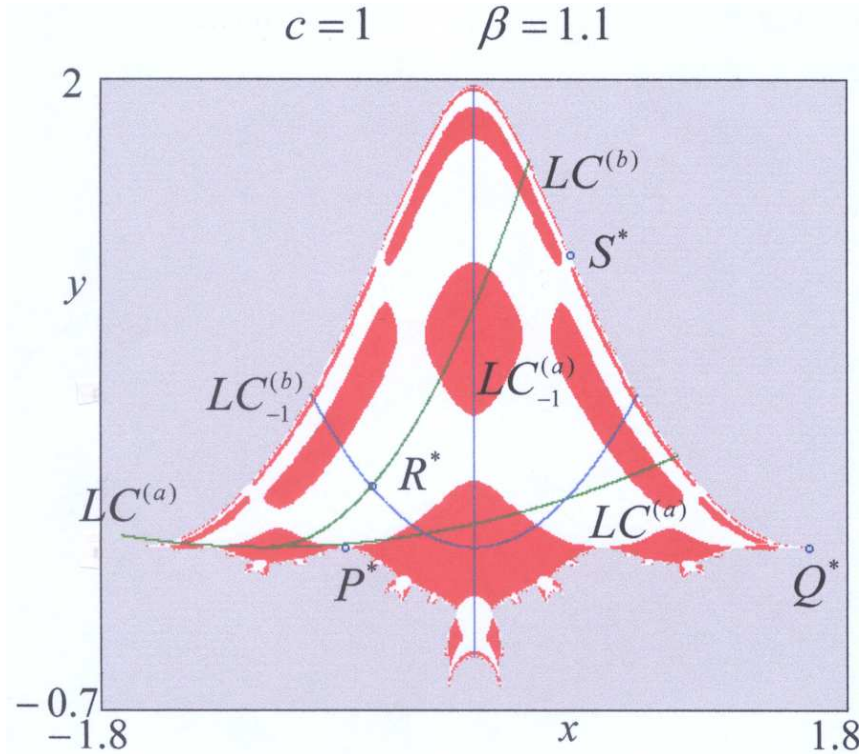

(a)

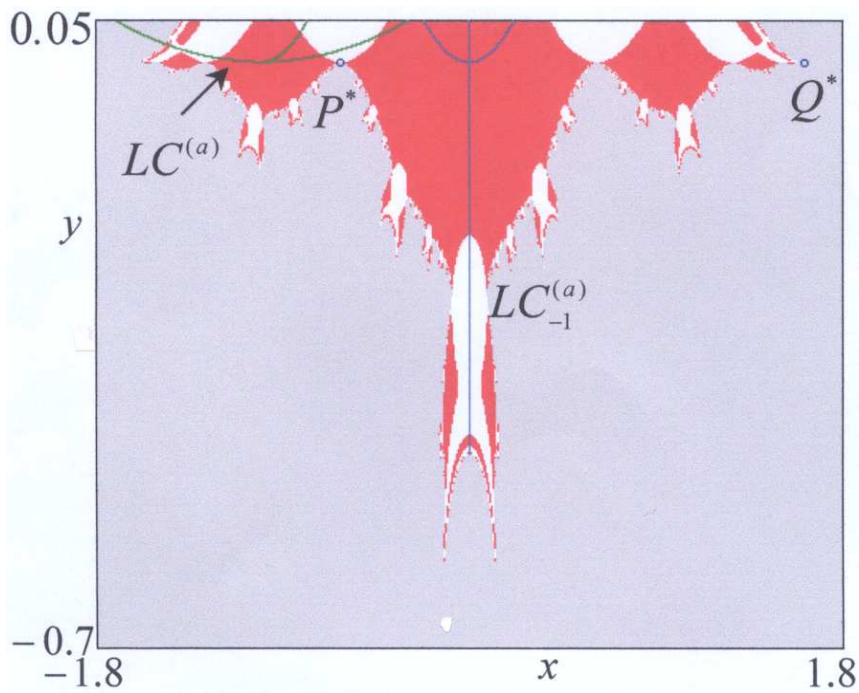

(b)

Fig. 6. (a) The set of points with bounded trajectories for the map T, when $\beta > 1$: as in Fig. 4, the attractors are the fixed point R^* and a 2-cycle, located on the x-axis. A portion of $LC^{(a)}$ enters in Π_+. (b) In the enlargement, this portion is more evident, as well as the "half-fractal" structure of the frontier in Π_-, due to the presence of infinitely many smooth arcs accumulating on a Cantor set of repelling cycles.

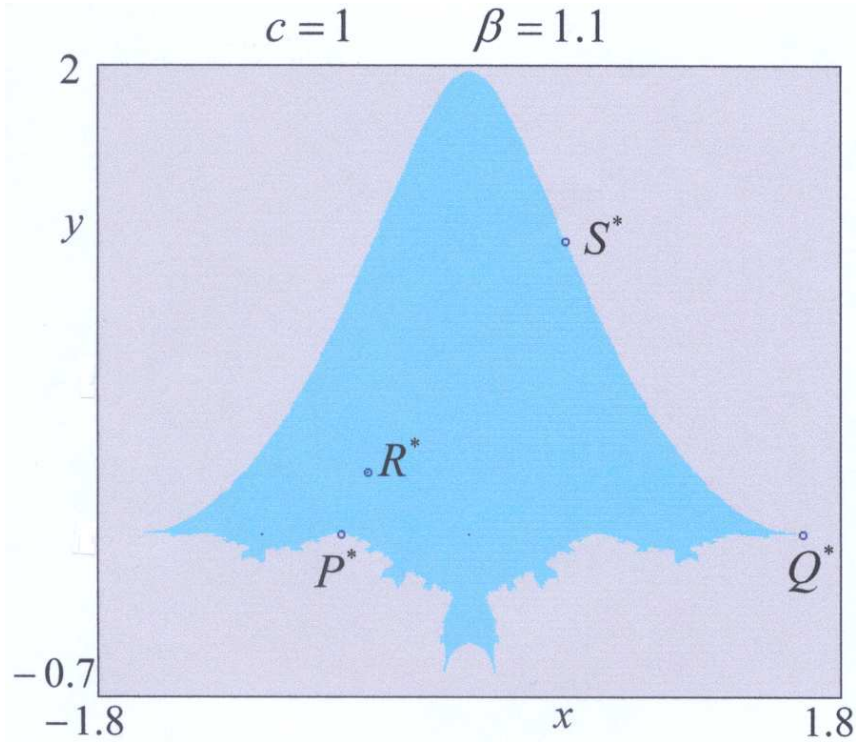

(a)

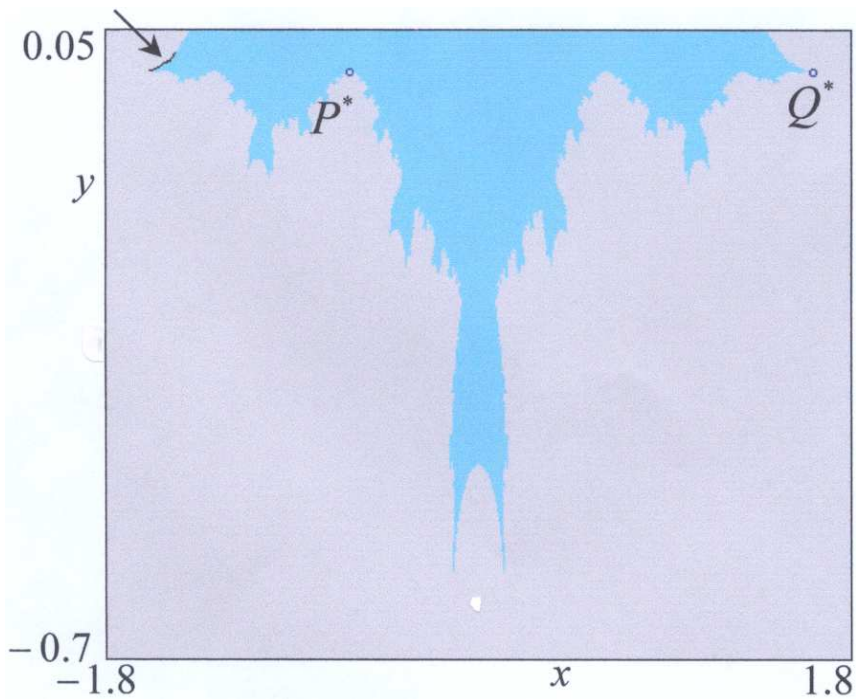

(b)

Fig. 7. (a) The same example as in Fig. 6: but the set of points with bounded trajectories is in light blue. This permits to better appreciate the boundary structure. (b) In the enlargement, an arrow indicates the small arcs in Π_+, whose preimages are the smooth arcs, giving rise to the "half-fractal" frontier.

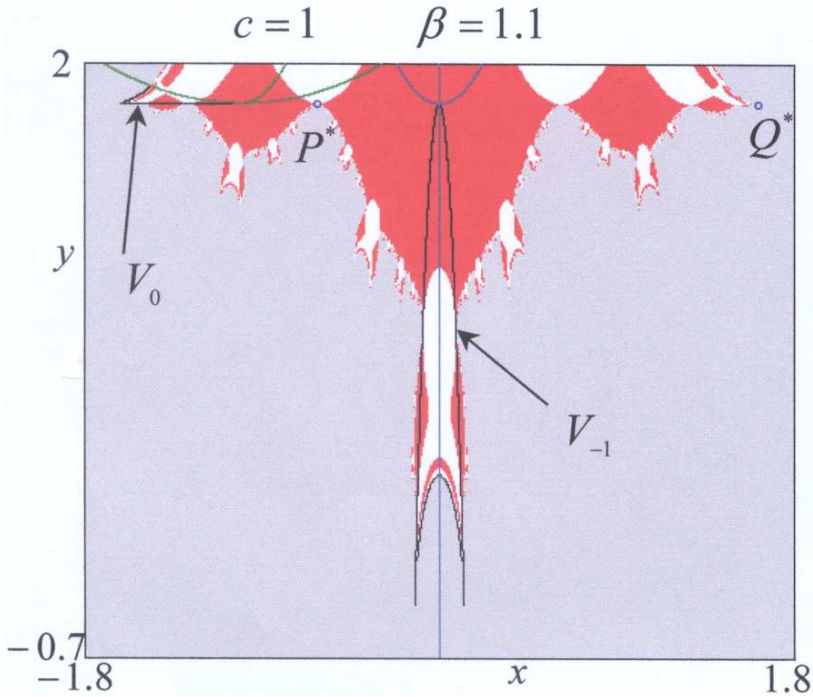

(a)

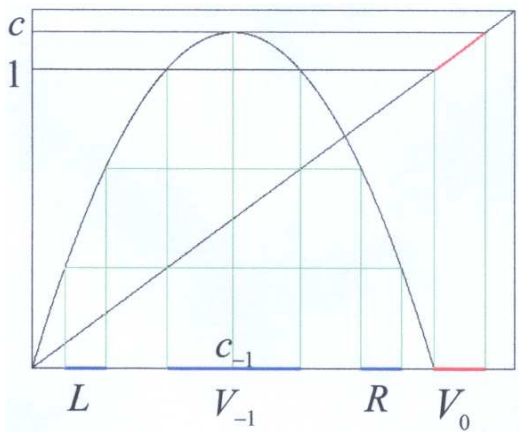

(b)

Fig. 8. (a) The enlargement of the frontier in Π_-, obtained for $\beta > 1$. The points of the region V_0 in the half-plane Π_+ have two preimages in Π_-, located at a side opposite to $LC_{-1}^{(a)}$, and merging on it. So that, saying V_{-1} the set of rank-1 preimages of V_0, $V_{-1} = V_{-1,L} \cup V_{-1,R}$. Also V_{-1} has two preimages in Π_-, one, $V_{-2,L}$, on the left of $LC_{-1}^{(a)}$ and the other, $V_{-2,R}$ on the right: the two sets, with the same shape of V_{-1} at the left of P^* ($V_{-2,L}$) and at the right of Q^* ($V_{-2,R}$). V_{-2} has two preimages ... and so on. (b) The analogous process of the one-dimensional logistic map with $\mu > 4$. The interval $V_0 = [1, c]$ has two rank-1 preimages located on opposite side with respect to c_{-1} and merging in it: the interval V_{-1} in figure. At its time, V_{-1} has two rank-1 preimages: the set L and R in the figure and so on.

of the self-similar structure of the Cantor set, due to the accumulation of infinitely many preimages on repelling cycles belonging to a repelling Cantor set.

This is immediately seen as β crosses 1, as shown in Figs. 6 and 7.

Let us consider the value $\beta = 1.1$, as in order to show the mechanism, any value $\beta > 1$ works well, in the same way as in the standard logistic map $x' = \mu x(1 - x)$, in order to show the existence of the surviving repeller Cantor set Λ in the

interval $[0, 1]$, any value $\mu > 4$ works equally well (see Fig. 8).

In our map T, for $\beta > 1$ the branch of $LC^{(a)}$ enters the positive half-plane Π_+, and, as remarked before, there are points of Π_- which are mapped in Π_+, while the property persists that any point $P \in \Pi_-$ has two distinct rank-1 preimages in Π_-. Thus there are points of Π_+ having preimages in Π_-, and from the properties of the foliation (i.e. of the inverses) the only points having this property are those of the region called V_0 in Fig. 8. The region V_0 above the x-axis is bounded by a portion of $LC^{(a)}$ and a portion of $\mathcal{F}$ belonging to Π_+ (made up of points belonging to the stable set of the saddle S^* located on the frontier). This area includes both points belonging to the basin of the stable fixed point $\mathcal{B}(R^*)$ (the white ones) and to the basin of the attracting cycle $\mathcal{B}(2-cycle)$ (the red ones). The two rank-1 preimages of V_0 are one on the right and one on the left of $LC^{(a)}_{-1}$, both in Π_- (see Fig. 8), constituting the set $V_{-1} = V_{-1,L} \cup V_{-1,R}$. Then V_{-1} has two distinct rank-1 preimages, one on the right and one on the left of $LC^{(a)}_{-1}$, the y-axis (see $V_{-2,L}$ and $V_{-2,R}$ in Fig. 8), and so on indefinitely:

$$
\begin{aligned}
T(\overline{\Pi}_-) &= \overline{\Pi}_- \cup V_0 \\
T^{-1}(V_0) &= V_{-1,L} \cup V_{-1,R} \\
T^{-2}(V_0) &= T^{-1}(V_{-1}) = V_{-2,L} \cup V_{-2,R} \\
&\dots
\end{aligned}
$$

The similarity of the process with that of the one-dimensional logistic map shown in Fig. 8 is now clear.

All the infinitely many repelling cycles existing at $\beta = 1$ on $\mathcal{F}$, persists also for $\beta > 1$. We can prove the existence of infinitely many cycles also for $\beta > 1$ by using a geometrical proof, which is the two-dimensional analogue of the one which is usual for the logistic map with $\mu > 4$, using neighborhoods instead of intervals, as described in the Appendix. However, by this geometrical proof we can only see that the infinitely many cycles exist and that the set which is invariant in Π_- has a Cantor-like structure, but we are not able to show that all are repelling (although we believe in this). This is left as an open problem for further researchers.

We note that now, for $\beta > 1$, the frontier $\mathcal{F}$ in Π_- is of so-called "half-fractal" type: it includes smooth arcs (all coming from the preimages of any order of V_{-1}, and the smooth part of the frontier includes a portion of the stable set of some saddle, and note that the saddle belongs to the positive half-plane), but the preimages of such smooth arcs are accumulating on a Cantor set of (repelling) cycles and with the property of self-similarity.

3.3. *Case* $\beta < 1$

As we have seen, crossing through $\beta = 1$ the basin boundary of T in Π_- undergoes the transition

$$\underset{\beta=1}{\text{hard-fractal}} \rightarrow \underset{\beta>1}{\text{half-fractal}}$$

and how about for $\beta < 1$?

As at $\beta = 1$ infinitely many repelling cycles exist on $\mathcal{F}$ and survive for $\beta > 1$, they must have been created as β tends to 1 on the left. In fact, looking at the frontier of the basin at values of β below 1, increasing β, we see a progressive increase of the fractal structure, through "islands" of red points, and the route to fractalization can be explained by the tools of noninvertible maps, associated with the properties of the critical curves and the foliation of the plane, as described in [Mira *et al.*, 1994] and [Mira *et al.*, 1996].

Let us consider the shape of the frontier at a parameter value far from the bifurcation value. As shown in Fig. 9 the geometrical shape of $\mathcal{F}$ for $\beta = 0.9$ seems quite smooth.

As β increases, approaching 1, the number of repelling cycles on $\mathcal{F}$ in Π_- increases. The qualitative change of the structure of the basin in Π_- is due to a sequence of "contact bifurcations" involving the frontier and the critical curve LC. The crossing of $\mathcal{F}$ through the critical curve $LC^{(a)}$ (see the enlargement in Fig. 10) gives rise to the appearance of "islands" of red basins, the first one around the critical curve $LC^{(a)}_{-1}$ and all its preimages of any rank. The preimages of the main portion around $LC^{(a)}_{-1}$ increases as β increases, as well as the preimages, giving rise to new bifurcations due to contacts and crossing of $LC^{(a)}$ and the same mechanism applies, creating new islands whose preimages are accumulating on more and more repelling cycles, approaching the fractal structure of $\mathcal{F}$, as can clearly be seen in Fig. 11.

At $\beta = 1$ all the islands will be in contact with each other on $\mathcal{F}$ leading to the true fractal structure existing at this value of β.

The one described above is the mechanism creating the hard-fractal structure which exists when $\beta = 1$ (as proven in Sec. 3.1) independently of the value of the parameter c. In order to show another

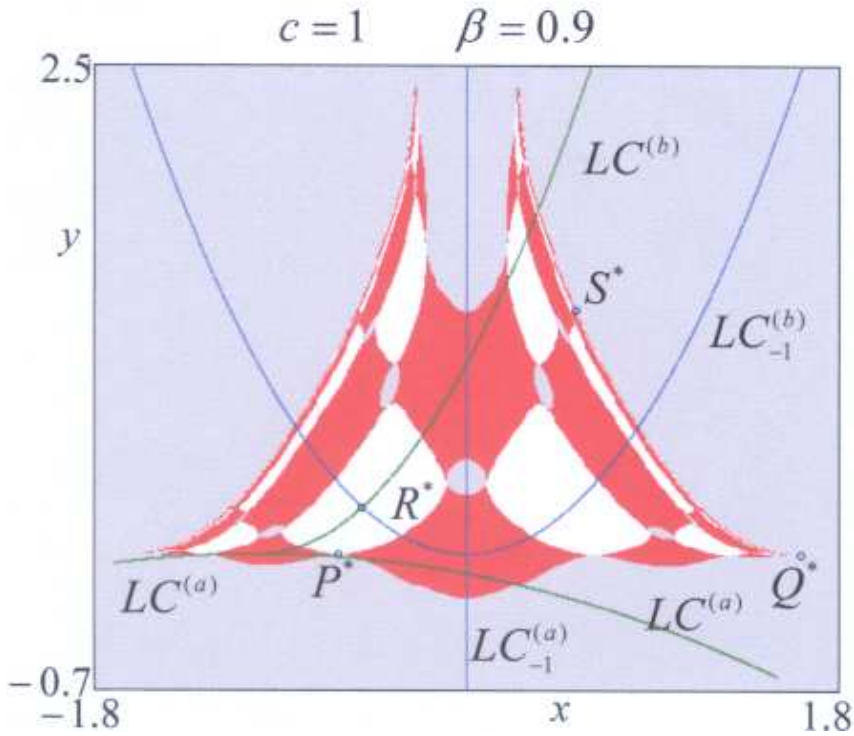

(a)

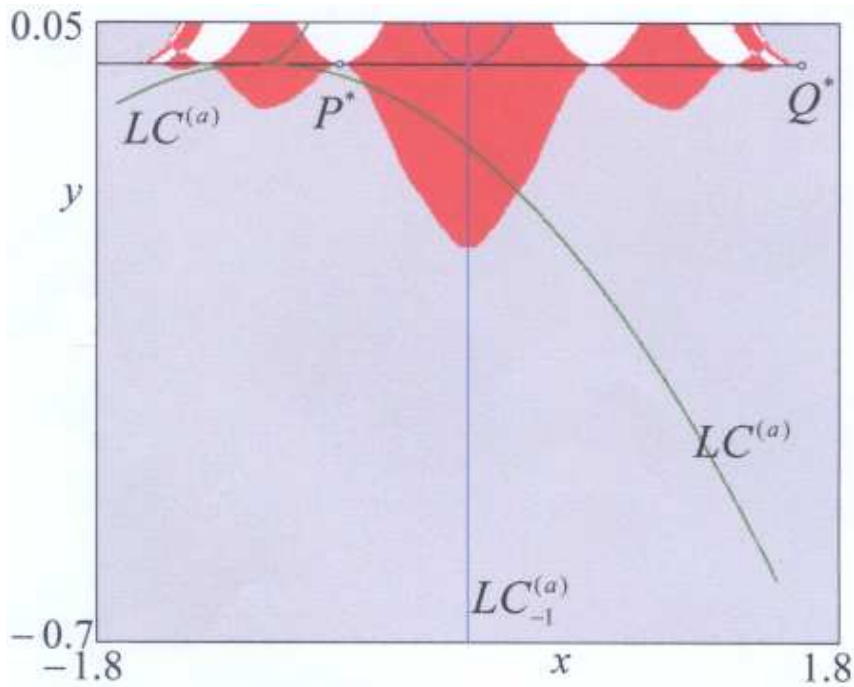

(b)

Fig. 9. (a) At $\beta = 0.9$, the boundary appears quite smooth. In the upper part, the basin is multiply connected, i.e. connected with holes, because near P^* there are gray points which have preimages. The presence of this region of points is due to a contact between the branch of $LC^{(a)}$ in the half-plane Π_- and the frontier of the basin. (b) In the enlargement, the region causing the appearance of holes in the basin is more evident. In the same figure we can also observe the quite smooth structure of the frontier in Π_-.

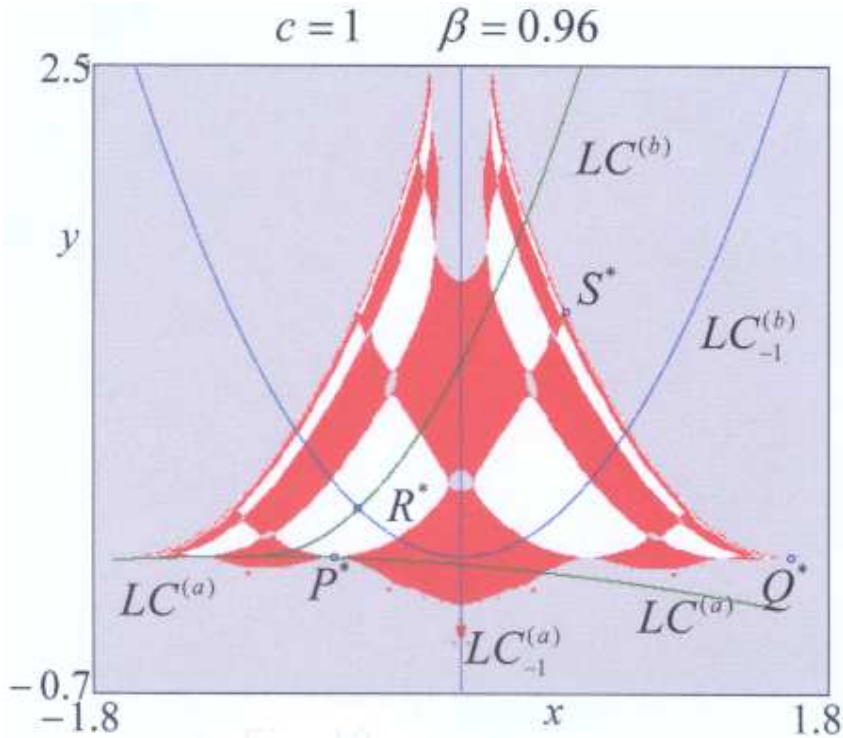

(a)

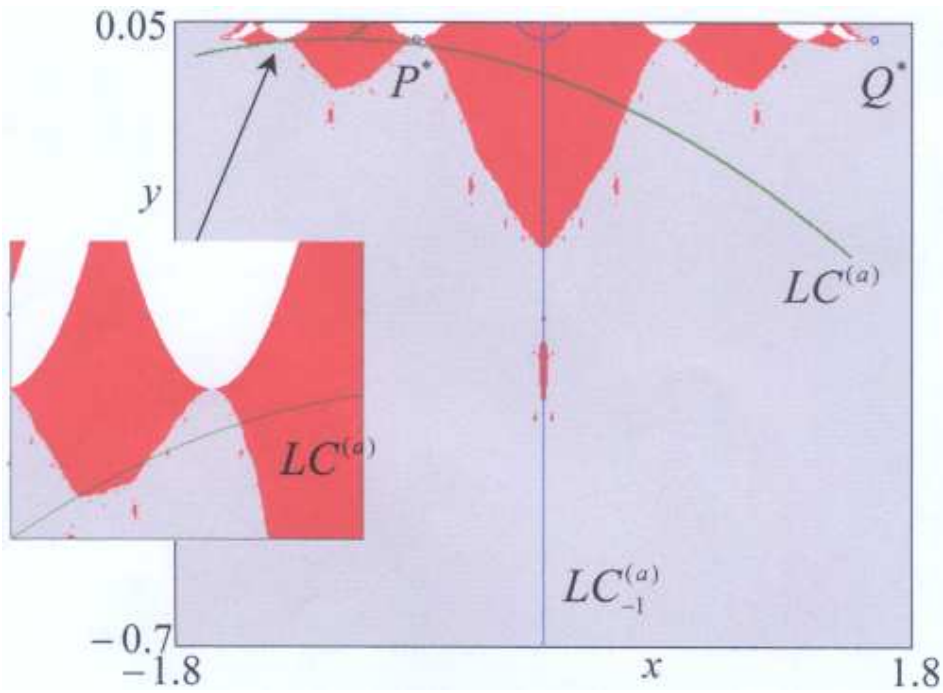

(b)

Fig. 10. (a) As β is increased, contact bifurcations, involving the frontier and the critical curve $LC^{(a)}$, of the same type as the one described in Fig. 9, give rise to the appearance of small red islands. (b) In the enlargement, observe the region of point which gives rise to the small islands and the "main island", i.e. the preimages of rank-1 of that region, located around $LC^{(a)}_{-1}$.

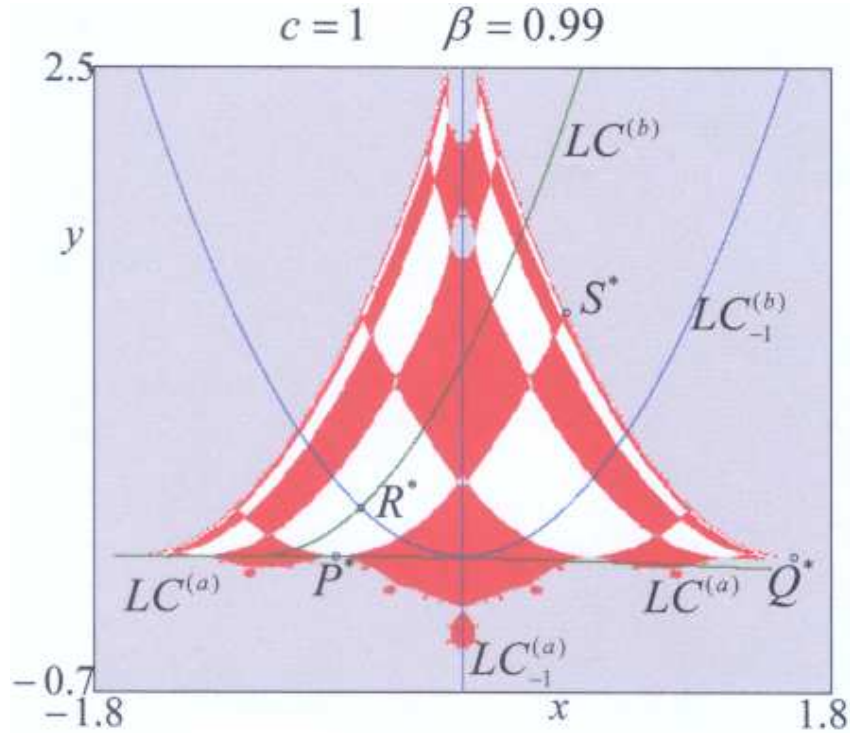

(a)

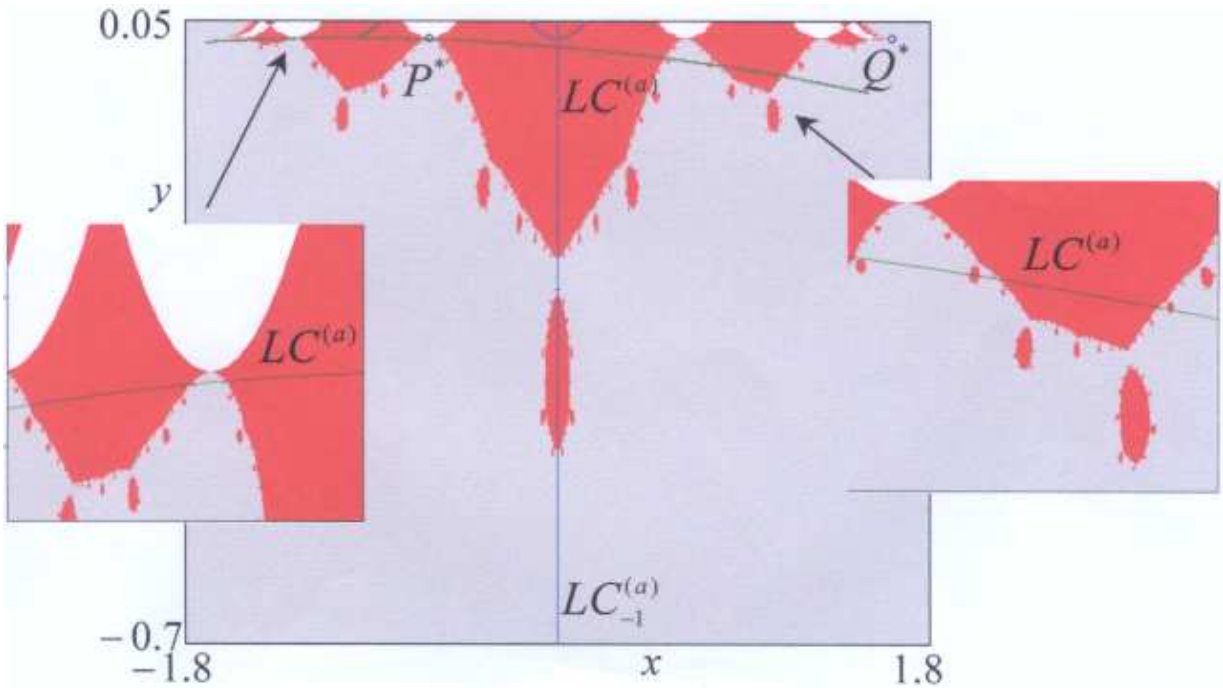

(b)

Fig. 11. (a) As β approaches 1, the preimages of the "main island" increases, as well as its preimages, giving rise to new islands (by new contact bifurcations) whose preimages are accumulating on more and more repelling cycles. (b) In the enlargement, one of the new contact bifurcations is indicated by an arrow, as well as the increased size of the region which gives rise to the process. The red islands are now very near to the frontier of the immediate basin and the "future" fractal structure is perceivable.

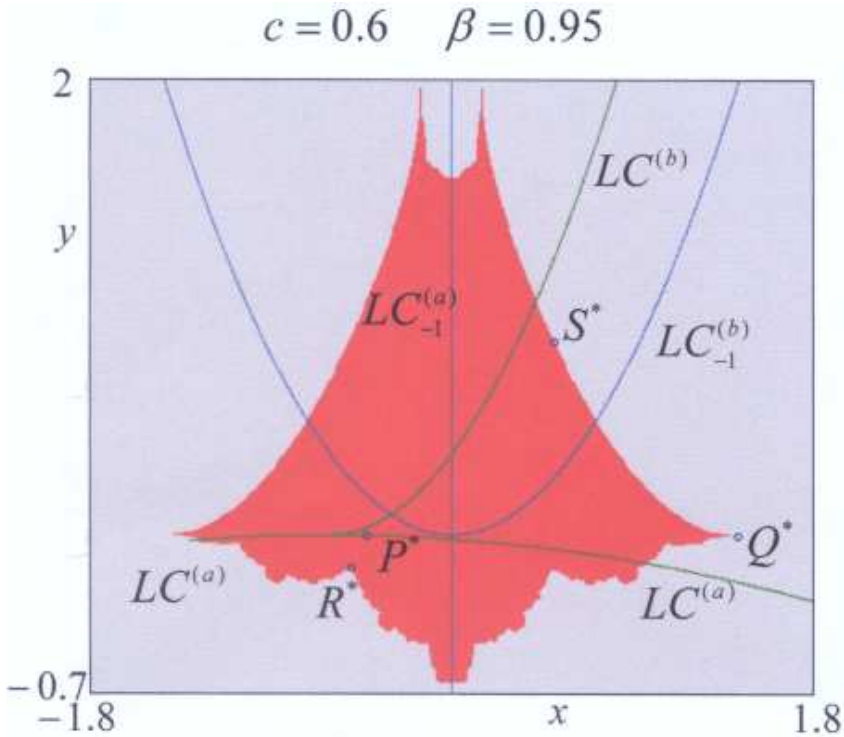

(a)

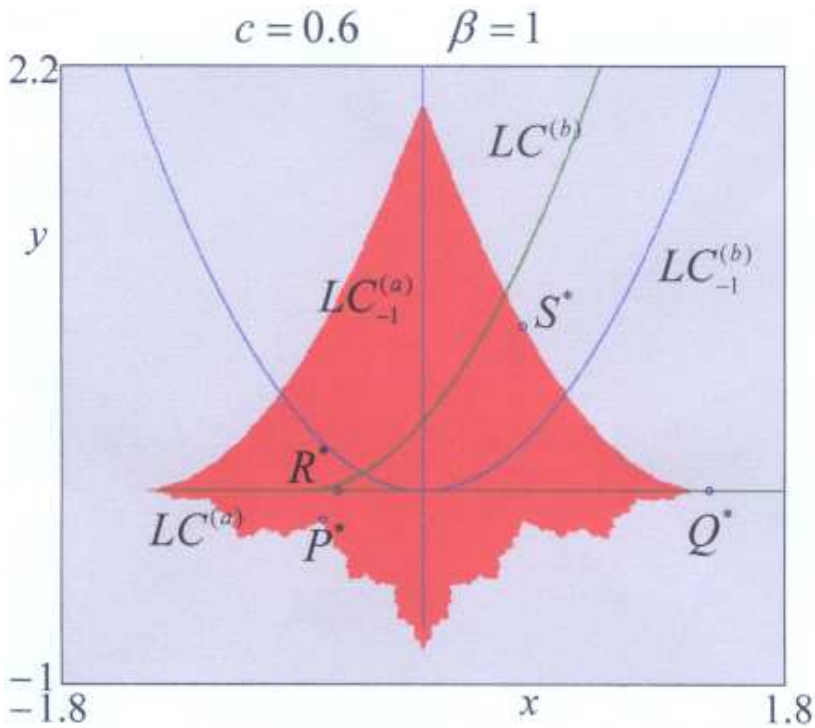

(b)

Fig. 12. A similar transition smooth — hard-fractal — half-fractal structure, as β crosses 1, is obtainable for different values of c. Here, we show the case $c = 0.6$ at which P^* is an attractive fixed point and R^* is a repelling fixed point located on the frontier in Π_-. (a) At $\beta < 1$, the frontier in Π_- is quite smooth. (b) At $b = 1$, the frontier has a "hard-fractal" structure. (c) At $b > 1$, the frontier has a half-fractal structure.

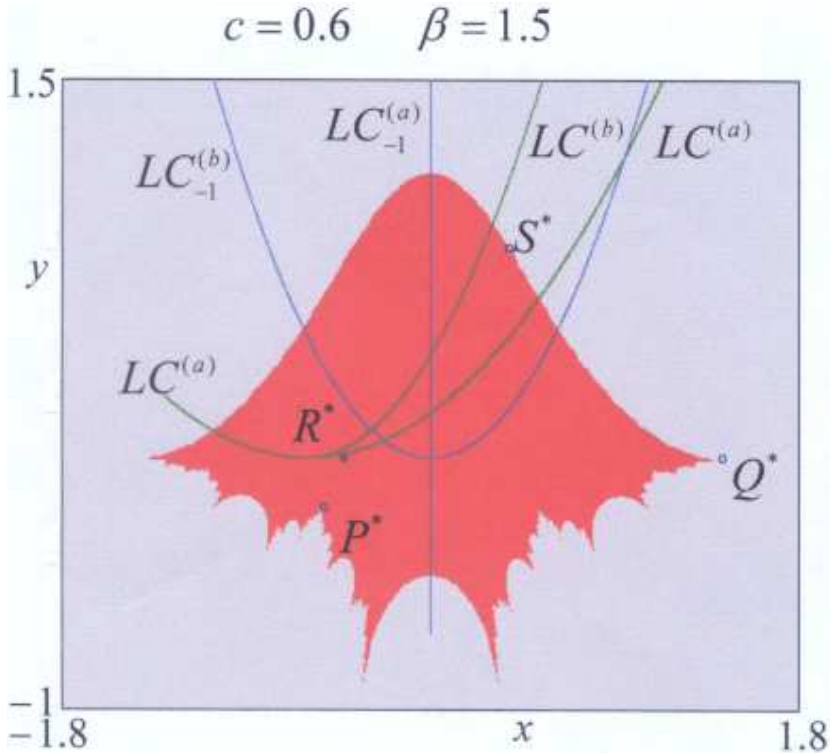

(c)

Fig. 12 (*Continued*)

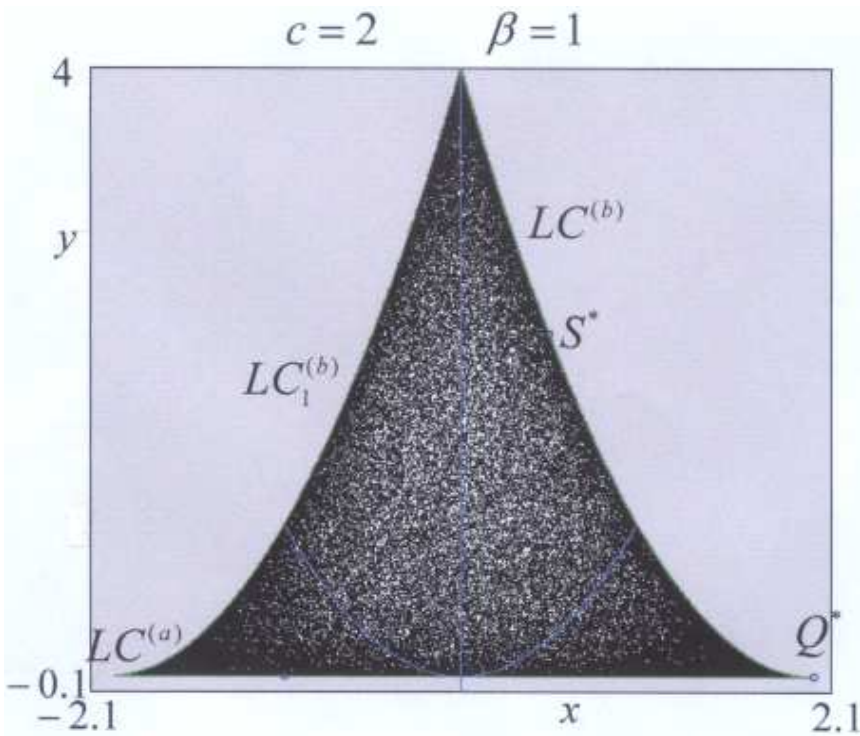

Fig. 13. For $c = 2$ the map T seems chaotic in the whole area bounded by critical curve segments, as the logistic map for $\mu = 4$.

example let us consider a lower value of c, for which the attractor on the x-axis is the stable fixed point P^*. We also have for the two-dimensional map T, that P^* is the only attractor, and the frontier of its basin is also the frontier of $\mathcal{B}_\infty$. The portion of $\mathcal{F}$ in Π_- from smooth for $\beta < 1$ becomes "hard-fractal" at $\beta = 1$, and "half-fractal" for $\beta > 1$.

In Fig. 12 the transition to half-fractal boundary can be observed as β crosses through 1.

Similarly we can reason at any value of c. In particular, we know that for $c = 2$ (equivalent to $\mu = 4$ for the logistic map) the Myrberg's map is chaotic in the interval bounded by the critical points $[c, c_1]$ and we have an analytical solution for the trajectories on the x-axis. At $\beta = 1$ also the two-dimensional map T seems chaotic in the whole area bounded by critical curve segments, see Fig. 13. We conjecture that also for T, there exist an analytical solution for the trajectories in this chaotic area, which may be determined via the "Schroeder mechanism" (see [Mira, 1987; Mira *et al.*, 1996]). We leave this as an open problem for those who are interested in these topics.

Acknowledgments

We thank seminar participants to the European Conference on Iteration Theory, ECIT-2000, for their comments. This work has been performed under the auspices of CNR, Italy and under the activity of the national research project "Dynamic Models in Economics and Finance", MURST, Italy.

References

Abraham, R., Gardini, L. & Mira, C. [1997] *Discrete Dynamical Systems in Two Dimensions* (Springer-Verlag, Berlin).

Agliari, A., Gardini, L., Delli Gatti, D. & Gallegati, M. [2000] "Global dynamics in a nonlinear model for the equity ratio," *Chaos Solit. Fract.* **11**, 961–985.

Gumowski, I. & Mira, C. [1980a] *Dynamique Chaotique. Transition Ordre-Desordre* (Cepadues, Toulouse).

Gumowski, I. & Mira, C. [1980b] *Recurrences and Discrete Dynamic Systems*, Lectures Notes in Mathematics, Vol. 809 (Springer-Verlag, Berlin).

Mira, C. [1987] *Chaotic Dynamics* (World Scientific, Singapore).

Mira, C., Fournier-Prunaret, D., Gardini, L., Kawakami, H. & Cathala, J. C. [1994] "Basin bifurcations of two-dimensional noninvertible maps: Fractalization of basins," *Int. J. Bifurcation and Chaos* **4**, 343–381.

Mira, C., Gardini, L., Barugola, A. & Cathala, J. C. [1996] *Chaotic Dynamics in Two-Dimensional Noninvertible Maps* (World Scientific, Singapore).

Appendix

In this Appendix we shall see that infinitely many cycles exist in Π_- for $\beta > 1$.

For $\beta \geq 1$ any point $P = (u, v) \in \Pi_-$ has two distinct rank-1 preimages in Π_-, one on the right and one on the left of the y-axis. We call these two inverses T_R^{-1} and T_L^{-1}:

$$T_R^{-1}(u, v) = (\sqrt{u + c - \xi}, \xi)$$
$$T_L^{-1}(u, v) = (-\sqrt{u + c - \xi}, \xi)$$

where

$$\xi = \frac{2(u + c) - \sqrt{4(u + c)^2 + |v|(5 - \beta)}}{(5 - \beta)}$$

The fact that any point always has two distinct rank-1 preimages in the same region is clearly an important peculiarity. This property is not "common" in two-dimensional maps, and it may be associated with the existence of chaotic dynamics in some invariant set.

The mechanism we use to prove the existence of infinitely many cycles in Π_- is the following.

Let us define the area bounded by $\mathcal{F} = \partial B_\infty$ in Π_- as the union of two closed sets: $U_L \cup U_R$ (bounded by portions of the coordinate axes and a portion of frontier $\mathcal{F}$). Then we have $T(U_L) \supseteq U_L \cup U_R$, $T(U_R) \supseteq U_L \cup U_R$, thus the Brower fixed point theorem holds and both U_L and U_R must contain a fixed point of T.

Then let $T^{-1}(U_R) = U_{LR} \cup U_{RR}$ and $T^{-1}(U_L) = U_{LL} \cup U_{RL}$. We have that $T^2(U_{LR}) \supseteq U_{LR}$, $T^2(U_{RR}) \supseteq U_{RR}$, $T^2(U_{LL}) \supseteq U_{LL}$ and $T^2(U_{RL}) \supseteq U_{RL}$, which implies that each of the four closed areas must include a fixed point of T^2, and U_{RL} being on the right of the y-axis, $T(U_{RL}) = U_L$ on the left, it follows that the fixed point of T^2 in this set U_{RL} cannot be a fixed point of T, so that it must be a cycle of period 2 for T.

Taking the preimages of U_{ij} for all the combinations of (i, j) with the two symbols L and R, we get sets $U_{i_1 i_2 i_3}$ (with all the combinations of (i_1, i_2, i_3) with the two symbols L, R), each of which satisfies $T^3(U_{i_1 i_2 i_3}) \supseteq U_{i_1 i_2 i_3}$ and the fixed point theorem applies. The existence of cycles of period 3 can be proved. In fact, by using the same reasoning as above, the sets with index (RLL, LLR, LRL) and the sets with index (RLL, LLR, LRL) must include periodic points belonging to cycles of period 3

(while the sets with index RRR and LLL include fixed points of T in U_R and U_L, respectively).

And so on, this process can never stop because any closed set in Π_- has two distinct rank-1 preimages in Π_-, at the step-k we have sets $U_{i_1 \dots i_k}$ (with all the combinations of $(i_1, \dots i_k)$ with the two symbols L, R), each of which satisfies $T^k(U_{i_1 \dots i_k}) \supseteq U_{i_1 \dots i_k}$ and the fixed point theorem applies. The existence in Π_- of cycles of period k can be proved by using the same reasoning as above.

We know that when $\beta = 1$ all the cycles in Π_- below the x-axis are on the frontier $\mathcal{F}$, while when $\beta > 1$ some cycle may be in the interior of the area in Π_- below the x-axis and bounded by the frontier $\mathcal{F}$, and in fact, they may belong to the internal frontier which separates the red points from the white ones. To see this we note that the cycles of T belonging to the coordinate axes are completely known, for example, at $\beta = 1.1$ on the x-axis the only cycles are two fixed points of T and one cycle of period 2, thus all the infinitely many cycles which we have proved to exist cannot belong to the portions of boundaries of the closed sets $U_{i_1 \dots i_k}$ which are preimages of any order of the coordinate axes. It follows that such cycles must be either in the interior or on the frontier of $U_{i_1 \dots i_k}$ which is a preimage of $\mathcal{F}$.

Let us close this Appendix recalling (as a numerical curiosity) a trick in order to detect any cycle of T in Π_- which is expanding, i.e. a repelling node or focus (it is the same that we apply in the case of the one-dimensional logistic map).

For example, in order to find the two cycles of period 3, starting from a point in Π_- we iterate the maps

$$T_R^{-1} \circ T_R^{-1} \circ T_L^{-1}$$

$$T_L^{-1} \circ T_L^{-1} \circ T_R^{-1}$$

In order to find the three cycles of period 4 we iterate the inverses in the order $RRRL$, $LLLR$, $RRLL$ (as the iteration of $RLRL$ gives the cycle of period 2, while iterating the inverses $RRRR$ we get the fixed point Q^* in U_R and iterating $LLLL$ the other fixed point P^* in U_L).

In general, starting from a point in Π_- and iterating the inverses in the following order:

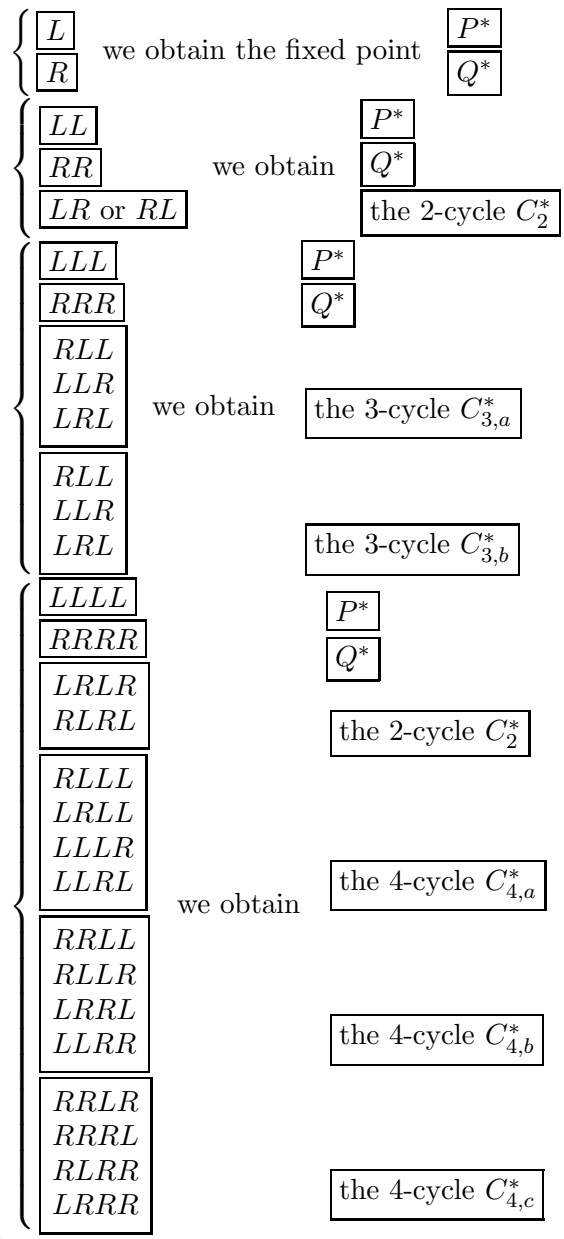

and so on.